

Towards High-Fidelity 3D Portrait Generation with Rich Details by Cross-View Prior-Aware Diffusion

Haoran Wei^{1*}, Wencheng Han^{1*}, Xingping Dong², Jianbing Shen^{1†}

¹SKL-IOTSC, CIS, University of Macau, ²School of Computer Science, Wuhan University

{hr.wei1998, wenchenghan, xingping.dong}@gmail.com, jianbingshen@um.edu.mo

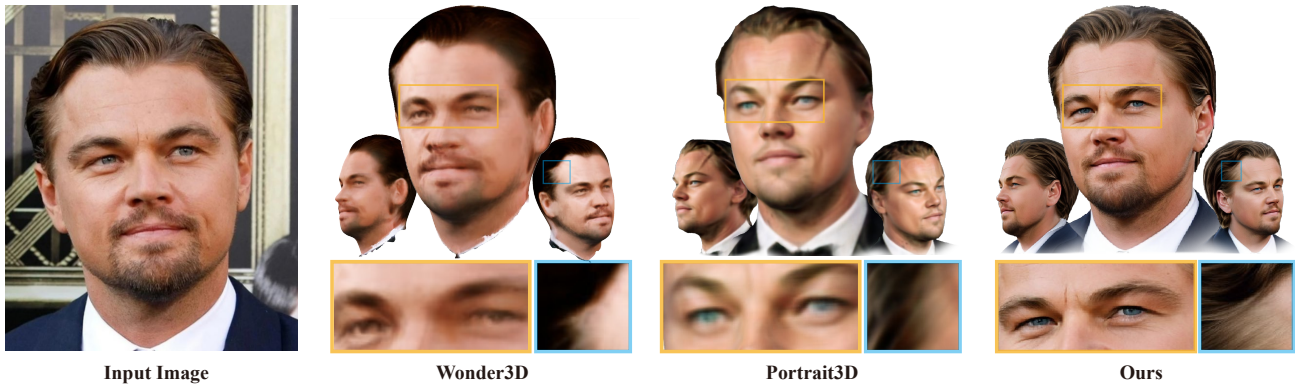


Figure 1. Our proposed **Portrait Diffusion** framework can generate high-quality detail-rich 3D portraits from a single reference portrait image. In comparison to SOTA methods **Wonder3D** [19] and **Portrait3D** [36], our approach achieves clearer and more detailed textures.

Abstract

Recent diffusion-based Single-image 3D portrait generation methods typically employ 2D diffusion models to provide multi-view knowledge, which is then distilled into 3D representations. However, these methods usually struggle to produce high-fidelity 3D models, frequently yielding excessively blurred textures. We attribute this issue to the insufficient consideration of cross-view consistency during the diffusion process, resulting in significant disparities between different views and ultimately leading to blurred 3D representations. In this paper, we address this issue by comprehensively exploiting multi-view priors in both the conditioning and diffusion procedures to produce consistent, detail-rich portraits. From the conditioning standpoint, we propose a Hybrid Priors Diffusion model, which explicitly and implicitly incorporates multi-view priors as conditions to enhance the status consistency of the generated multi-view portraits. From the diffusion perspective, considering the significant impact of the diffusion noise distribution on detailed texture generation, we propose a Multi-View Noise Resampling Strategy integrated within the optimization process leveraging cross-view priors to enhance representation

consistency. Extensive experiments demonstrate that our method can produce 3D portraits with accurate geometry and rich details from a single image. The project page is at <https://haoran-wei.github.io/Portrait-Diffusion>.

1. Introduction

The generation of realistic 3D portraits from a single image [7, 10, 20, 35, 39] has become an important focus in computer vision and graphics, with broad applications in augmented reality, virtual reality, video conferencing, and gaming [14, 18, 45]. The most straightforward approach involves training GAN models [1, 47] on extensive portrait datasets to directly produce 3D representations. However, acquiring such training data can be costly and technically challenging, leading to failures in generating high-fidelity 360° full-head portraits [7, 8] and often resulting in a lack of diversity in the outputs.

To address these limitations, recent developments [24, 26, 30, 31, 46] leverage text-to-image diffusion priors [5, 41, 44], which exhibit stronger generalization capabilities and higher generation quality, to produce novel perspectives.

* Equal contribution. † Corresponding author: Jianbing Shen.

tives. Most approaches incorporate additional priors, such as reference image latents [42, 50], ID features [13, 28], and view embeddings [28], to enhance the consistency between new perspectives and the primary viewpoint. Subsequently, they commonly employ Score Distilling Sampling (SDS) loss [25] to distill these 2D priors into 3D representations, ensuring consistent 3D generation.

However, in single-image 3D portrait generation, these methods still face challenges: generated portraits often appear over-smoothed and fail to capture detailed textures like hair strands, as illustrated in Fig. 1, limiting their practical applications. We attribute this issue to the insufficient consideration of cross-view consistency during the diffusion process, resulting in significant disparities between different views. This 2D inconsistency results in blurred 3D output by SDS optimization. Although these methods attempt to improve consistency by incorporating additional priors, they rely solely on diffusion attentions to implicitly convey these priors. This reliance results in a lack of explicit constraints, leading to inconsistent status across different viewpoints. Moreover, the diffusion procedure is inherently stochastic; even with the same conditions, a diffusion model can generate varied representations due to randomly sampled noises. By using view-independent procedures with purely random noise in diffusion, these methods overlook the impact of stochasticity on representation consistency. Consequently, these inconsistencies in status and representation jointly result in over-smoothed 3D models when optimized under the SDS loss, which enforces 3D consistency and continuity in sacrifice of texture details.

To address these issues, we propose fully exploiting cross-view priors in both the conditioning and diffusion procedures to enhance multi-view consistency, thus yielding detail-rich 3D portraits, as showcased in Fig. 1. From a conditioning perspective, we propose Hybrid Priors Diffusion Model (HPDM). Our approach seeks to transfer and utilize cross-view prior information in both explicit and implicit ways to control the novel view generation. In an explicit manner, we begin by employing geometric priors to map pixels from the current view to the next, providing an explicit reference to dominate the generation process. Given that this reference encompasses only a limited overlapping region and contains artifacts introduced through perspective transformations, we further propose to utilize the robust modeling capabilities of attention mechanisms to mitigate these deficiencies. These mechanisms capture finer texture and geometry priors and implicitly transfer these priors into the control conditions, ensuring a more comprehensive and precise guidance for the portrait status of novel viewpoint.

From a diffusion procedure perspective, our goal is to manage randomness in adjacent viewpoints so that they can share detailed, consistent representations. To achieve this, we introduce a Multi-View Noise Resampling Strat-

egy (MV-NRS) integrated into the SDS loss, which manages each view’s noise distribution by passing cross-view priors. MV-NRS consists of two main components: first, a shared anchor noise initialization that leverages geometric priors to establish a preliminary representation; and second, an anchor noise optimization phase, where we resample and update the anchor noise based on denoising gradient consistency prior to progressively align the representations during the SDS optimization.

To summarize, our main contributions are as follows:

- We developed a Portrait Diffusion pipeline consisting of GAN-prior Initialization, Portrait Geometry Restoration, and Multi-view Diffusion Refinement modules to generate rich-detail 3D portraits.
- We designed a Hybrid Priors Diffusion Model that emphasizes both explicit and implicit integration of multi-view priors to impose conditions, aiming to enhance the consistency of multi-view status.
- We introduced a Multi-View Noise Resampling Strategy integrated within the SDS loss to manage randomness across different views through the transmission of cross-view priors, thereby achieving fine-grained consistent representations.
- Through extensive experiments, we show that our proposed pipeline successfully achieves high-fidelity 3D full portrait generation with rich details.

2. Related Work

One-shot 3D Generation 3D GANs [4, 11, 27, 40, 43, 48] have made significant strides in advancing one-shot 3D object generation by enhancing both quality and efficiency. GRAM [6] enhanced efficiency through point sampling on 2D manifolds, and GET3D [12] integrated differentiable rendering with 2D GANs to efficiently generate detailed 3D meshes. For improving 3D consistency, Geometry-aware 3D GAN [3] used a hybrid architecture to maintain multi-view consistency, while GRAM-HD [37] employed super-resolution techniques to address inconsistency issues. Despite these advances, limited datasets constrain the prior distribution, and acquiring high-quality data remains costly.

Recently, methods leveraging 2D diffusion prior [2, 21, 21–23, 33, 34, 49] for generating 3D objects have gained traction [9, 16, 26, 32, 38, 46]. Dreamfusion [24] introduces a loss mechanism based on probability density distillation for optimizing parametric image generators. Dream-Craft3D [29] employs view-dependent diffusion models for coherent 3D generation, using Bootstrapped Score Distillation to enhance textures. Make-It-3D [30] uses 2D diffusion models as perceptual supervision in a two-stage process, enhancing textures with reference images. Make-it-Vivid [31] focuses on automatic texture generation from text instructions, achieving quality outputs in UV space. These advancements underscore the promise of diffusion priors in

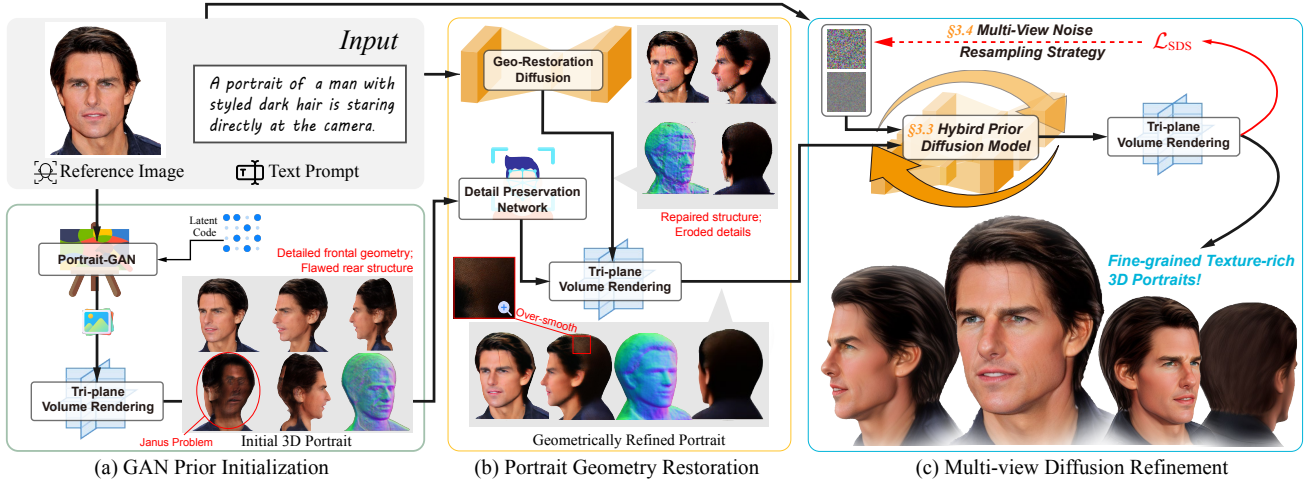


Figure 2. **The Portrait Diffusion Framework.** This framework comprises three integral modules. *GAN-prior Portrait Initialization*, employs existing Portrait GAN priors to derive initial tri-plane NeRF features from frontal-view portrait images. *Portrait Geometry Restoration*, is focused on reconstructing the geometry using these initialized tri-planes. *Multi-view Diffusion Texture Refinement*, transforms coarse textures into detailed representations.

achieving multi-view consistency in 3D object generation.

One-shot 3D Portrait Generation In 3D portrait synthesis, Yin et al. [47] enhanced 3D GAN inversion using facial symmetry and depth-guided pseudo labels for better structural consistency and texture fidelity. PanoHead [1] creates 360° portraits with a two-stage registration process using tri-mesh neural volumetric representation.

Benefiting from diffusion priors, diffusion models significantly enhance 3D portrait synthesis by enabling detailed zero-shot full head generation. Portrait3D [36] uses 3DPortraitGAN to produce 360° canonical portraits, addressing “grid-like” artifacts with a pyramidal tri-grid representation and improving details through diffusion model fractional distillation sampling. DiffusionAvatars [17] combine a diffusion-based renderer with a neural head model, using cross-attention for consistent expressions across angles. Another Portrait3D framework [13] by Hao et al. emphasizes identity preservation in avatars across three phases: geometry initialization, sculpting, and texture generation, employing ID-aware techniques. While many of these methods utilize SDS and incorporate ID and normal information for enhanced representation, they often struggle to fully utilize multiple priors across viewpoints, leading to texture issues like over-smoothing or artifacts.

3. Methods

In this section, we first analyze the limitations of existing methods and give our motivations (Sec. 3.1). Next, we provide an overview of our pipeline, including GAN Prior Initialization Module, Portrait Geometry Restoration Module and Multi-view Diffusion Texture Refinement Module (Sec. 3.2). We then focus on the Multi-view Diffusion

Texture Refinement Module, emphasizing both Multi-view Status Consistency (Sec. 3.3) and Multi-view Representation Consistency (Sec. 3.4) to achieve consistent multi-view generation achieving fine texture fidelity in 3D portrait.

3.1. Preliminary

Existing diffusion-based methods for generating 3D objects predominantly utilize Score Distillation Sampling (SDS) loss [25] to distill 2D diffusion priors into 3D representations. This process can be formulated as follows:

$$\Phi^* = \arg \min_{\Phi} (\mathcal{L}_{\text{SDS}}(\Phi; \theta) + \mathcal{L}_{\text{ref}}(\Phi; I^{\text{ref}})) \quad (1)$$

where Φ denotes the parameters of the 3D model, $\mathcal{L}_{\text{SDS}}(\Phi; \theta)$ represents the SDS loss using a diffusion model parameterized by θ , and $\mathcal{L}_{\text{ref}}(\Phi; I^{\text{ref}})$ is a loss computed from reference image I^{ref} . The SDS loss can be formulated as:

$$\begin{aligned} \nabla_{\Phi} \mathcal{L}_{\text{SDS}} &= \mathbb{E}_{t,v,\epsilon} \left[w_t (\epsilon_{\theta}(z_{t,v}, t, c) - \epsilon) \cdot \nabla_{\Phi} \mathcal{R}_{\Phi}(v) \right] \\ z_{t,v} &= \sqrt{\alpha_t} z_v(\Phi) + \sqrt{1 - \alpha_t} \epsilon, \quad \epsilon \sim \mathcal{N}(0, \mathbf{I}), \end{aligned} \quad (2)$$

where $z_{t,v}$ is a noisy latent representation obtained by combining the image latents $z_v(\Phi)$, which is rendered from viewpoint v by Φ , with random noise ϵ ; $\epsilon_{\theta}(z_{t,v}, t, c)$ is a diffusion UNet model that predicts the noise component at each time step t , conditioned on c . w_t and α_t are weights, and \mathcal{R} is rendering function.

From (2), the SDS loss aggregates the denoising gradients from all v to the 3D model parameters Φ . When the denoising distributions across viewpoints are inconsistent, the SDS loss will produce over-smoothed representations to minimize the overall loss by averaging conflicting gradients, sacrificing the details of each perspective. The denoising function ϵ_{θ} is influenced by both the conditions c

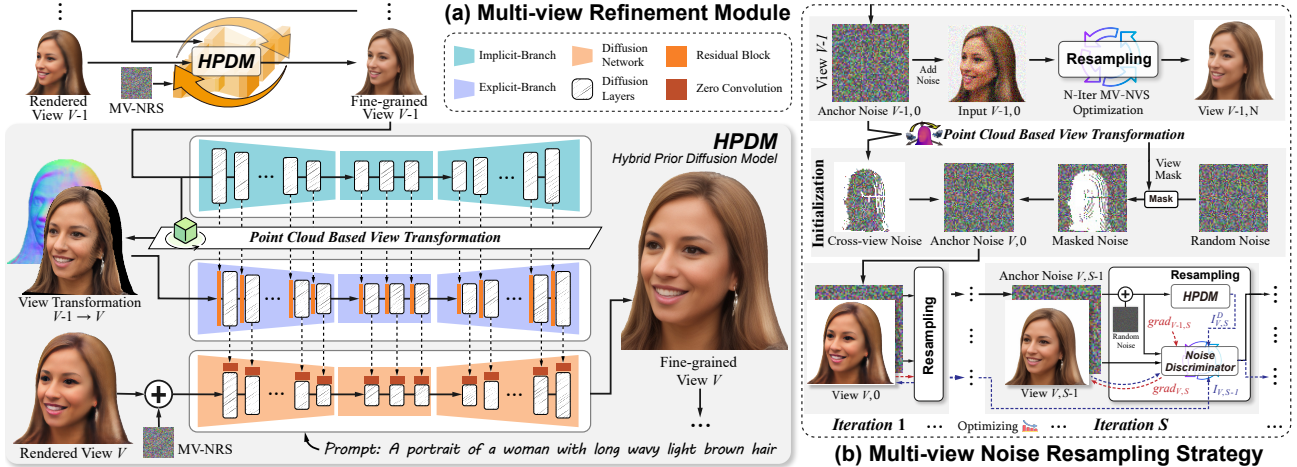


Figure 3. The presentations of our proposed **Hybrid Priors Portrait Diffusion model** (a) and **Multi-View Noise Resampling Strategy** (b). HPDM is designed to leverage various multi-view priors in a hybrid manner to condition the new view synthetic process for more consistent status. NV-NRS is designed to transfer cross-view priors to control the diffusion noise distribution for representations alignment.

and the distribution of noise ϵ from each viewpoint, making them essential for the quality of the 3D representation.

However, previous methods did not fully leverage multi-view priors to effectively control both conditions c and noise ϵ . This resulted in inconsistent multi-view denoising, making them impossible to generate detailed 3D textures. Although some of these methods incorporate additional priors like ID features to enhance the condition, they rely solely on implicit priors transfer through embeddings and attention mechanisms within the diffusion, while lacking explicit guidances. Therefore, they are unable to effectively constrain the portrait status across different views. Additionally, these methods focus merely on enhancing conditions c and overlook the significant influence of ϵ on detailed representations. As a result, the mutually independent multi-view noise adding procedure leads to a lack of fine-grained alignment in denoising gradients.

3.2. Detail-Rich Portrait Diffusion

Our Portrait Diffusion framework for high-fidelity detail-rich 3D portrait generation is illustrated in Fig. 2. It consists of three major modules:

GAN-Prior Initialization Module utilizes GAN priors learnt from large-scale offline multi-view portrait images to initialize a tri-plane representation, as shown in Fig. 2 (a). This tri-plane offers preliminary geometry and texture, facilitating the subsequent training process.

In our method, we employ a NeRF, parameterized by Ψ , as our 3D model. Initialization plays a critical role in the quality of NeRF models. Standard initialization, such as using a central sphere, often produce excessively smooth geometries with insufficient details. Therefore, a high-quality initialization can significantly benefit the subsequent optimization process. Inspired by Portrait 3D [13], we utilize

GAN priors to initialize NeRF representations. Specifically, we utilize SOAT GAN method [7] to generate triplane features from a frontal image. This process can be formalized as:

$$\begin{aligned} T_{\text{init},I} &= \mathcal{G}_{\psi_{\text{enc}}}(I) \\ \Psi_{\text{init},I} &= \{T_{\text{init},I}, \psi_{\text{dec}}, \psi_{\text{SR}}\} \end{aligned} \quad (3)$$

where G denotes the GAN, which is parameterized by the encoder ψ_{enc} , decoder ψ_{dec} and superresolution ψ_{SR} parameters, T represents triplane features and $\Psi_{\text{init},I}$ represents the initialized NeRF parameters for image I .

While GAN-generated portraits effectively capture frontal details, they are constrained by the lack of 360° priors, leading to missing geometry at the back and the Janus issue. Therefore, we devise a Portrait Geometry Restoration module to further repair the geometry for the 3D portrait.

Portrait Geometric Restoration Module is designed to fix the structure of the initialized tri-plane with Diffusion priors. It employ diffusion models to deliver high-quality, generalized priors, and introduces a Detail Preservation Block that effectively preserves the details from the initialized priors, as shown in Fig. 2 (b).

Directly optimizing the triplane can lead to the erosion of initialized details; therefore, we employ a Detail Preservation Module that features a small UNet to transform the initialized tri-plane into the desired tri-plane instead. The core idea is to propagate gradients across the entire tri-plane through conv layers, thereby effectively leveraging the global priors. It considers the overall distribution of the initialized priors and subtly adjusts it to maintain coherence through optimizing the UNet parameters.

The Neural Geo Restoration process is divided into two steps: First, by pretraining on a large dataset of portraits with SDS loss and Geo-Restoration Diffusion, the UNet,

parameterized by ϕ , acquires generalized structure generation capabilities:

$$\phi_{\text{pre}}^* = \arg \min_{\phi} \sum_{I \in \mathcal{D}} L_{\text{SDS}}(\text{UNet}_{\phi}(T_{\text{init},I}); \Psi_{\text{init},I}), \quad (4)$$

where ϕ denotes the parameters of the UNet.

Then, it is fine-tuned on a specific portrait to adapt perfectly to its unique structure:

$$\begin{aligned} \phi_{\text{fit},I}^*, \psi_{\text{dec},I}^* &= \arg \min_{\phi, \psi_{\text{dec}}} L_{\text{SDS}}(\text{UNet}_{\phi}(T_{\text{init},I}), \\ &\psi_{\text{dec}}; T_{\text{init},I}, \psi_{\text{SR}}), \quad \text{s.t. } \phi(0) = \phi_{\text{pre}}^* \end{aligned} \quad (5)$$

$$\begin{aligned} T_{\text{fit},I}^* &= \text{UNet}_{\phi_{\text{fit},I}^*}(T_{\text{init},I}) \\ \Psi_{0,I} &= \{T_{\text{fit},I}^*, \psi_{\text{dec},I}^*, \psi_{\text{SR}}\}, \end{aligned} \quad (6)$$

where $\Psi_{0,I}$ represents the startup NeRF parameters for texture generation of image I , $\phi(0)$ represents the initial value of ϕ for fine-tuning. More training details are presented in Sec. 7.

Through these two modules, we have achieved geometrically refined portraits; however, intricate texture details are lost due to multi-view inconsistency training. To address this, we have designed a Multi-view Diffusion Refinement Module utilizing this geometric prior.

Multi-view Diffusion Refinement Module generates fine-grained 3D texture based on the reconstructed geometry through our Hybrid Priors Diffusion Model and Multi-View Noise Resampling Strategy, as shown in Fig. 2 (c).

This method is designed to thoroughly utilize various priors from both conditioning and diffusion procedure perspectives to improve consistency. From a conditioning perspective, the Hybrid Priors Diffusion Model effectively leverages and transmits multi-view priors both explicitly and implicitly—utilizing additional conditioning branches parameterized by θ^{Ex} and θ^{Im} —to enhance the consistency of novel viewpoints. From a diffusion procedure perspective, we acknowledge the role of noise in conveying detailed multi-view priors and devised a Multi-View Noise Resampling Strategy integrated within the SDS loss ($\mathcal{L}_{\text{SDS}}^{\text{MV-NRS}}$), which adjusts the distribution of resampled diffusion noise ϵ^{Rs} for fine-grained representations alignment. Through the $\mathcal{L}_{\text{SDS}}^{\text{MV-NRS}}$ and $\theta^{\text{Ex}}, \theta^{\text{Im}}$, we can generate detail-rich portraits:

$$\begin{aligned} \Psi_I^* &= \arg \min_{\Psi} (\mathcal{L}_{\text{SDS}}^{\text{MV-NRS}}(\Psi, \epsilon^{\text{Rs}}; \{\theta, \theta^{\text{Ex}}, \theta^{\text{Im}}\}) \\ &+ \mathcal{L}_{\text{ref}}(\Psi; I)), \quad \text{s.t. } \Psi(0) = \Psi_{0,I} \end{aligned} \quad (7)$$

3.3. Multi-view Status Consistency

Fig. 3 (a) presents our **Hybrid Prior Diffusion Model (HPDM)**, which focuses on leveraging multi-view priors in a hybrid manner to condition the novel view synthesis process for more consistent portrait status. Initially,

we leverage explicit priors by providing reference images to dominate the generation process, offering direct control and constraints. Following inpainting tasks, we introduce our *Explicit-Branch*. This branch takes the image projected from the driving view to the target view as an explicit reference and extends it to fill in the invisible areas.

To generate this reference, we convert the driven view image I_{v_i} into a colored 3D point cloud P_{v_i} using the NeRF-rendered depth map D_{v_i} . Then, a reference image of target view is rendered from this colored point cloud:

$$I_{v_{i+1}}^{\text{Proj}} = \mathcal{R}_{P_{v_i}}(v_{i+1}, I_{v_i}) \quad (8)$$

Besides, the segmentation mask S_{v_i} is similarly rendered onto the target view as an auxiliary mask condition $S_{v_{i+1}}^{\text{Proj}}$. The $z_{v_{i+1}}^{\text{Proj}}$, obtained by encoding $I_{v_{i+1}}^{\text{Proj}}$ from an VAE, along with the $S_{v_{i+1}}^{\text{Proj}}$ are fed into the diffusion UNet.

The diffusion UNet, following the inpainting method [15], is a adapted version of a pretrained diffusion UNet. In this adaptation, the cross-attention components are removed to focus entirely on the reference. Features from this UNet are injected into the frozen layers of the original diffusion UNet layer by layer with zero convs, allowing for dense, pixel-level control over the generation process:

$$\begin{aligned} \epsilon_{\theta}(z_t, t, y)_l &= \epsilon_{\theta}(z_t, t, y)_l \\ &+ w^{\text{Ex}} \cdot \mathcal{Z}(\epsilon_{\theta}^{\text{Ex}}([z^{\text{Proj}}, S^{\text{Proj}}, z_t], t)_l), \end{aligned} \quad (9)$$

where l denotes the l layer of the UNet, \mathcal{Z} denotes zero conv and w^{Ex} denotes control weight.

However, since the reference cannot guide all areas and the degraded priors during the view transformation, relying solely on such explicit priors transfer would introduce noises into control signals.

To address this, we aim to implicitly leverage priors to compensate for these deficiencies. To enhance texture priors, we integrated a second branch, *Implicit-Branch*, for lossless texture understanding, and designed a res-block to semi-explicitly pass this understanding to the Explicit-Branch. In detail, this branch is a copy of a Explicit-Branch that directly takes the driving image $I_{v_{i-1}}$ as input. To ensure effective transfer of these priors to the Explicit-Branch, we first explicitly rendering Implicit-Branch latents into the target view and then implicitly integrating them into the Explicit-Branch through res-blocks with zero-convs. We opt for simple res-blocks rather than complex transformers, benefiting from the spatial prior alignment provided by explicit geometric projection. The design of the res-blocks is detailed in the Sec. 6. This process can be expressed as:

$$\begin{aligned} &\epsilon_{\theta}^{\text{Ex}}([z_{v_i}^{\text{Proj}}, S_{v_i}^{\text{Proj}}, z_{t,v_i}], t)_l \\ &= \text{Res}[\epsilon_{\theta}^{\text{Ex}}([z_{v_i}^{\text{Proj}}, S_{v_i}^{\text{Proj}}, z_{t,v_i}], t)_l, \\ &\mathcal{R}_{P_{v_{i-1}}}(v_i, \epsilon_{\theta}^{\text{Im}}([z_{v_{i-1}}, z_{t,v_i}], t)_l)] \end{aligned} \quad (10)$$

Additionally, to compensate for the geometric artifacts in the explicit reference, we incorporate the geometric prior of the current view. To ensure that the generation aligns with the current geometry, the rendered coarse image I^R and normal map N^R are included as additional conditions within the Explicit-Branch. To enhance the geometry without overshadowing the reference texture, we once again employ a res-block to implicitly merge these conditions with the reference in latent space:

$$z^{\text{Proj}} = \text{Res}(z^{\text{Proj}}, \text{VAE}(N^R, I^R)) \quad (11)$$

3.4. Multi-view Representation Consistency

Although the aforementioned conditions can enhance the consistency of the generation status, considering the stochastic nature of diffusion process, it is crucial to align the generated representations by controlling the noise sampling distribution for each viewpoint. Therefore, we propose utilizing cross-view priors to identify the optimal noise distribution for each perspective, ensuring that multi-view representations are well-aligned and remain clear. To this end, we develop a **Multi-View Noise Resampling Strategy (MV-NRS)** within the SDS Loss. MV-NRS consists of two steps: *anchor noise initialization* and *anchor noise optimization*, as shown in Fig. 3 (b).

To identify these noise distributions, we begin by pinpointing a specific set of multi-view noise, denoted as anchor noise $\epsilon_{v_1:v_N}^{\text{Ac}}$, to ensure the generated images under these noises are initially more closely aligned. Subsequently, we perform resampling based on this anchor noise set, facilitating an initial alignment of the generated distributions. The resampled ϵ^{Rs} , with a small variance σ^2 , follows the distribution:

$$\epsilon^{\text{Rs}} \sim \mathcal{N}(\sqrt{1 - \sigma^2} \epsilon^{\text{Ac}}, \sigma^2 \mathbf{I}) \quad (12)$$

We recognize that the output of the 2D diffusion model demonstrates both invariance to linear transformations and robustness to small-scale nonlinear transformations. Consequently, it exhibits a degree of invariance to small-range viewpoint changes, which can be considered as local linear transformations. Therefore, by aligning the inputs according to the viewpoints, we can ensure that the outputs align as well. Since the input of the UNet consists of a combination of rendered image latents and noises, we only need to align the noises. To achieve this, we just lift the driven view noise into a point cloud and render it onto the target views:

$$\begin{aligned} \epsilon_{v_{i+1},0}^{\text{Ac}} &= \mathcal{R}_{P_{v_i,0}}(\epsilon_{v_i,0}^{\text{Ac}}, v_{i+1}) + \epsilon^{\text{rand}} \odot M_{v_{i+1},0}^{\text{void}} \\ \epsilon_{v_0,0}^{\text{Ac}} &\sim \mathcal{N}(0, \mathbf{I}), \quad \epsilon^{\text{rand}} \sim \mathcal{N}(0, \mathbf{I}), \end{aligned} \quad (13)$$

where $s = 0$ denotes the initial training iteration and M is a mask that indicates the locations of voids in the rendered noise. Compared to random noise initialization, this method

uses cross-view priors to build noise, enabling the capture of some small-scale noise distributions that are almost impossible to obtain through pure random sampling, particularly when the multi-view generative distributions are far apart.

Next, since the initial representations may not be perfectly aligned, we utilize multi-view gradient consistency to gradually finetune the anchor noises during the SDS training. Specifically, we have designed a Resampling Retention Strategy:

In each training iteration s , we first resampled a noise $\epsilon_{v_i,s}^{\text{Rs}}$ according to (12). Then, we decide whether to keep the resampled noise for updating the anchor noise by utilizing the multi-view gradient consistency score. The key idea is compute the gradients obtained from both the resampled noise and the anchor noise, and then assess their similarity with the gradients from the driven viewpoint. By comparing these similarities, we can determine whether to retain the resampled noise.

In detail, for $\epsilon_{v_i,s}^{\text{Rs}}$, we first compute the loss between a rendered image $I_{v_i,s}^R$ and denoised image $I_{v_i,s}^D$ from $\epsilon_{v_i,s}^{\text{Rs}}$, then backpropagate it to get the gradient $grad_{v_i,s}^D$:

$$\mathcal{L}_{v_i,s}^D = \mathcal{L}_I(I_{v_i,s}^R, I_{v_i,s}^D) \quad (14)$$

$$grad_{v_i,s}^D = \mathcal{BP}_{\Psi_{s-1}}(\mathcal{L}_{v_i,s}^D) \quad (15)$$

The cosine similarity is used to evaluate the consistency between this gradient and the applied gradient of the driven view $grad_{v_{i-1},s}$:

$$S_{v_i,s}^D = \frac{grad_{v_i,s}^D \cdot grad_{v_{i-1},s}}{\|grad_{v_i,s}^D\| \|grad_{v_{i-1},s}\|} \quad (16)$$

Similarly, for anchor noise $\epsilon_{v_i,s-1}^{\text{Ac}}$, we direct use the $I_{v_i,s-1}$ of previous training iteration to compute the gradient $grad_{v_i,s-1}^P$ the corresponding score $S_{v_i,s-1}^P$.

If $S_{v_i,s}^D > S_{v_i,s-1}^P$, the resampled noise is superior over the anchor noise in terms of gradient consistency. Therefore, we update the anchor noise and treat $I_{v_i,s}^D$ as the current target image, $grad_{v_i,s}^D$ as the current applied gradient. Conversely, we retain the anchor noise and target image, using the corresponding gradient instead:

$$I_{v_i,s}, \epsilon_{v_i,s}^{\text{Ac}}, grad_{v_i,s} = \begin{cases} I_{v_i,s}^D, \epsilon_{v_i,s}^{\text{Rs}}, grad_{v_i,s}^D & \text{if } S_{v_i,s}^D > S_{v_i,s-1}^P \\ I_{v_i,s-1}, \epsilon_{v_i,s-1}^{\text{Ac}}, grad_{v_i,s-1}^P & \text{otherwise} \end{cases} \quad (17)$$

After calculations for all viewpoints, we aggregate the gradients across all views, denoted as $Grad_s$. Finally, we update the 3D model in the current training iteration:

$$Grad_s = \sum_v grad_{v_i,s} \quad (18)$$

$$\Psi_s = \Psi_{s-1} + \alpha_s \cdot Grad_s \quad (19)$$

For more detailed MV-NRS process, refer to Sec. 7.

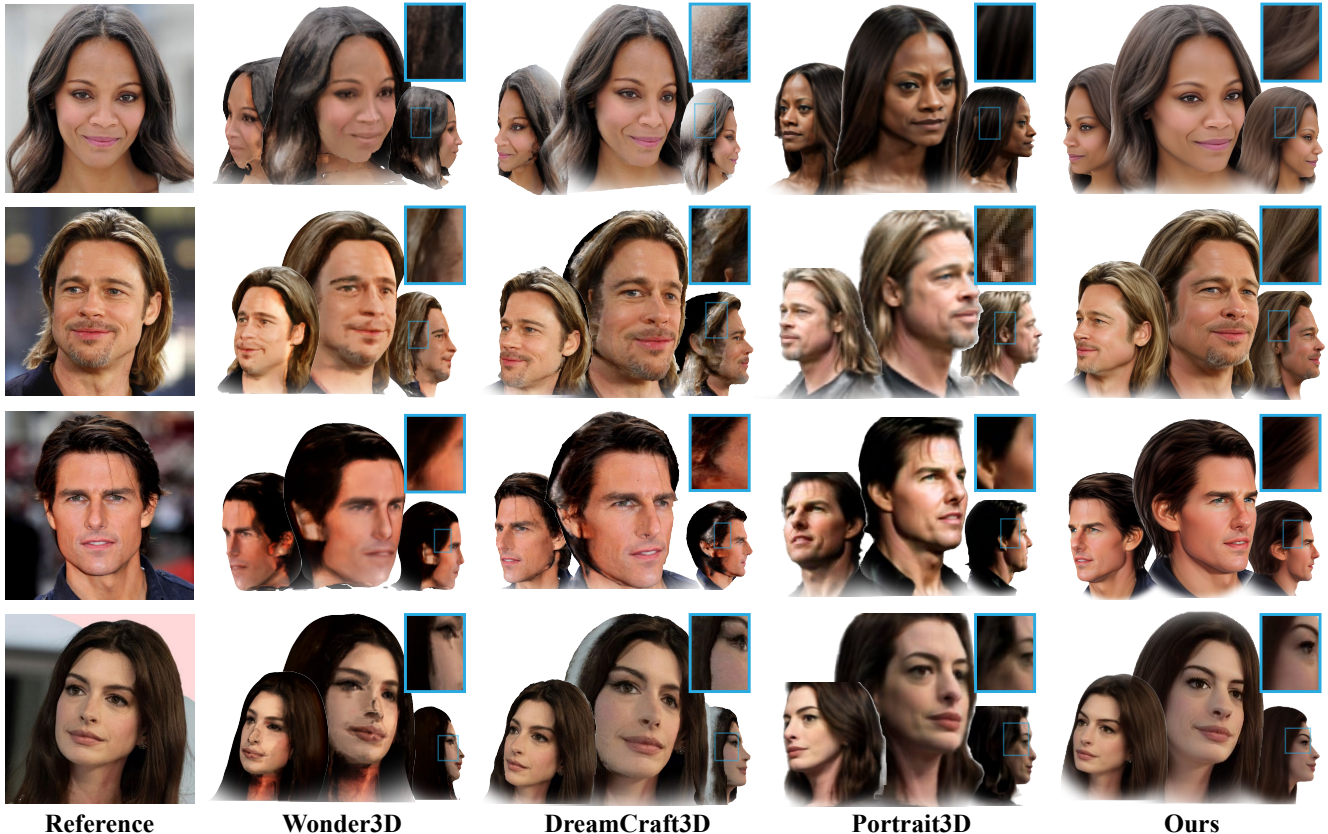


Figure 4. Qualitative comparison to SOTA approaches: Portrait3D [36], Wonder3D [19], and DreamCraft3D [29]. Our method presents the most photorealistic 3D portraits, with the most detailed textures in the face and hair strands. *Zoom in for more detailed insights.*

4. Experiments

4.1. Implementation Details

We employ triplane features with a resolution of 128×128 and a total of 96 channels, resulting in a rendered image resolution of 512×512 . During the geometry restoration phase, we randomly sampling viewpoints across a full 360° azimuth and a pitch angle ranging from -30° to 30° for SDS training. In the texture restoration phase, we reconstruct images using 13 fixed viewpoints. The training of our HPDM uses synthetic dataset from GANs methods. In addition to these fixed perspectives, we randomly sample additional viewpoints and apply a multi-step denosing SDS loss (image-supervised) to improve rendering quality between the fixed viewpoints. All our experiments were conducted on a single A100 GPU. For more hyperparameters and training details, please refer to the Sec. 7.

4.2. Qualitative Results

We compare our results with those from open-sourced SOTA approaches: Portrait3D [36], DreamCraft3D [29], and Wonder3D [19]. Notably, Portrait3D is a text-to-3D method; in our case, we bypass the text-to-image step by

directly providing the reference image.

From Fig. 4, it can be observed that the models generated by Wonder3D exhibit excessive smoothness and show a distinctly toy-like texture. While DreamCraft3D demonstrates some improvements, it completely loses reasonable texture in the profile view. Compared to the previous methods, Portrait3D can produce visually appealing models; however, it experiences identity variation issues and exhibits overly blurred textures and some artifacts in regions with complex hair patterns (e.g. the hair ends in the second row). In contrast, our model demonstrates the strongest fidelity and texture quality. We achieve an identity that is highly consistent with the reference and generating hair texture style that align appropriately with the reference. Furthermore, we can distinctly showcase the texture of nearly every strand of hair. Therefore, our proposed Portrait Diffusion surpasses SOTA methods and achieves the most detailed textures in 3D portraits.

4.3. Quantitative Evaluation

To comprehensively evaluate our generated head models, we employed three complementary metrics: CLIP-I for overall structural consistency, LPIPS for perceptual similar-

Method	CLIP-I \uparrow	LPIPS \downarrow	ID \uparrow
Portrait3D	0.9956	0.4258	0.1899
Wonder3D	0.9943	0.4377	0.3057
DreamCraft3D	0.9969	0.4064	0.2314
Portrait Diffusion	0.9986	0.3616	0.3440

Table 1. Quantitative comparison to SOTA approaches.

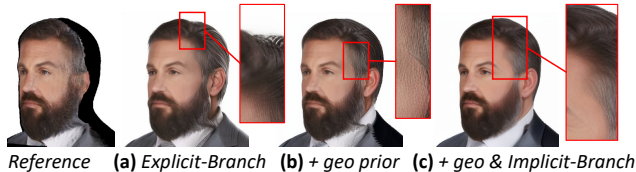


Figure 5. Visual Results for Ablation study on Hybrid Priors Diffusion Model.

ity, and ID metric for identity preservation. For the CLIP-I metric, we compute the cosine similarity of the CLIP features between images. The evaluation is implemented by rendering images from five distinct viewpoints: front, left-frontal, left, right-frontal, and right. All five rendered images are included in the calculations for the three metrics alongside the reference image.

The Tab. 1 shows our quantitative evaluation results. Our method achieves the highest CLIP-I score, indicating that our 3D portrait exhibits the greatest semantic consistency across various viewpoints. Additionally, we obtain the lowest LPIPS loss, demonstrating that our portraits maintain the most visually consistent appearance from different views. Furthermore, our approach achieves the highest ID score, confirming that our portraits exhibit the strongest identity consistency across multiple perspectives. The highest quantitative metrics indicate that our approach surpasses the generative quality of SOTA methods.

4.4. Ablation Study

Effectiveness of the Hybrid Priors Diffusion Model. The Fig. 5 illustrates the visual results of the ablation study conducted to evaluate the effectiveness of the Hybrid Priors Diffusion Model. Panel (a) displays results of conditioning only with Explicit-Branch, which aligns corresponding areas in the reference but reveals numerous deficiencies in both structure and texture. Panel (b) demonstrates the results achieved by incorporating geometric priors into the model. This addition fosters a more harmonious and unified geometry, significantly improving the overall shape fidelity of the 3D portrait. However, there are still texture striped artifacts present. Panel (c) further incorporates texture priors (Implicit-Branch), effectively eliminating all striped texture artifacts and showcasing exquisite details. This validates the effectiveness of our approach in leveraging multiple types of priors.

Effectiveness of the Multi-View Noise Resampling Strat-

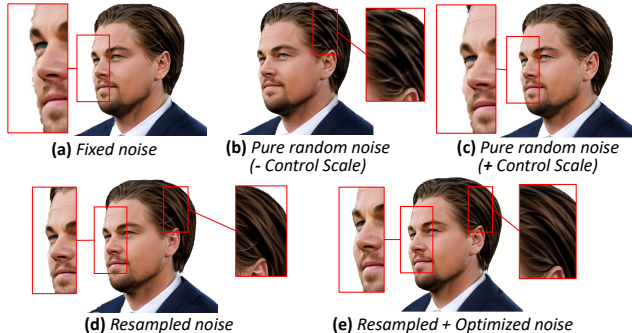


Figure 6. Visual Results for Ablation study on Multi-View Noise Resampling Strategy.

egy. The visual results displayed in Fig. 6 illustrate the ablation study conducted to assess the effectiveness of the Multi-View Noise Resampling Strategy (MV-NRS). Panel (a) displays the results with fixed noise during SDS loss, which lack randomness and reveal artifacts resulting from misalignment. Panel (b) and (c) show the outcomes with completely random noise: Panel (b) utilizes a lower control scale, resulting in a smoother generation representation while maintaining consistency, while Panel (c) applies a higher control scale, overly constraining the generation distribution and resulting in issues similar to Panel (a), though to a lesser degree. Panel (d) presents the results of MV-NRS without anchor noise optimization, resembling the outcomes in Panel (c). This demonstrates that without continuously updating anchor noise, alignment cannot be effectively improved. Panel (e) presents our complete MV-NRS, which avoids both excessive smoothing and artifacts. These results demonstrate that our MV-NRS, through both resampling and optimization, enables the fine-grained generation of detailed textures using HPDM.

5. Conclusion

We introduced a Portrait Diffusion pipeline that generates detail-rich 3D full portraits. This pipeline consists of three main modules, including a GAN-prior Initialization module, a Portrait Geometric Restoration module and a Multi-view Diffusion Refinement Module. Our Multi-view Diffusion Refinement Module incorporates a Hybrid Priors Diffusion model that effectively leverage multi-view priors for consistent status, and a Multi-View Noise Resampling Strategy to ensure consistent representations during the optimization. Qualitative and Quantitative assessments have shown that portraits produced by our pipeline exhibit superior detail and realism compared to state-of-the-art alternatives. Our Portrait Diffusion pipeline sets a new standard in 3D portrait generation, offering unparalleled texture detail and fidelity, and paving the way for future developments in computer vision, graphics, and digital art.

References

- [1] Sizhe An, Hongyi Xu, Yichun Shi, Guoxian Song, Umit Y. Ogras, and Linjie Luo. Panohead: Geometry-aware 3d full-head synthesis in 360deg. In *Proceedings of the IEEE/CVF Conference on Computer Vision and Pattern Recognition*, pages 20950–20959, 2023. 1, 3
- [2] Chenjie Cao, Chaohui Yu, Yanwei Fu, Fan Wang, and Xiangyang Xue. Mvinpainter: Learning multi-view consistent inpainting to bridge 2d and 3d editing. *arXiv preprint arXiv:2408.08000*, 2024. 2
- [3] Eric R. Chan, Connor Z. Lin, Matthew A. Chan, Koki Nagano, Boxiao Pan, Shalini De Mello, Orazio Gallo, Leonidas J. Guibas, Jonathan Tremblay, and Sameh Khamis. Efficient geometry-aware 3d generative adversarial networks. In *Proceedings of the IEEE/CVF Conference on Computer Vision and Pattern Recognition*, pages 16123–16133, 2022. 2
- [4] Hansheng Chen, Jiatao Gu, Anpei Chen, Wei Tian, Zhuowen Tu, Lingjie Liu, and Hao Su. Single-stage diffusion nerf: A unified approach to 3d generation and reconstruction. In *Proceedings of the IEEE/CVF International Conference on Computer Vision*, pages 2416–2425, 2023. 2
- [5] Ciprian Corneanu, Raghudeep Gadde, and Aleix M Martinez. Latentpaint: Image inpainting in latent space with diffusion models. In *Proceedings of the IEEE/CVF Winter Conference on Applications of Computer Vision*, pages 4334–4343, 2024. 1
- [6] Yu Deng, Jiaolong Yang, Jianfeng Xiang, and Xin Tong. Gram: Generative radiance manifolds for 3d-aware image generation. In *Proceedings of the IEEE/CVF Conference on Computer Vision and Pattern Recognition*, pages 10673–10683, 2022. 2
- [7] Yu Deng, Duomin Wang, and Baoyuan Wang. Portrait4d: Learning one-shot 4d head avatar synthesis using synthetic data. In *Proceedings of the IEEE/CVF Conference on Computer Vision and Pattern Recognition*, 2024. 1, 4
- [8] Yu Deng, Duomin Wang, and Baoyuan Wang. Portrait4d-v2: Pseudo multi-view data creates better 4d head synthesizer. *arXiv preprint arXiv:2403.13570*, 2024. 1
- [9] Lihe Ding, Shaocong Dong, Zhanpeng Huang, Zibin Wang, Yiyuan Zhang, Kaixiong Gong, Dan Xu, and Tianfan Xue. Text-to-3d generation with bidirectional diffusion using both 2d and 3d priors. In *Proceedings of the IEEE/CVF Conference on Computer Vision and Pattern Recognition*, pages 5115–5124, 2024. 2
- [10] Michail Christos Doukas, Stefanos Zafeiriou, and Viktoriia Sharmanska. Headgan: One-shot neural head synthesis and editing. In *Proceedings of the IEEE/CVF International conference on Computer Vision*, pages 14398–14407, 2021. 1
- [11] Aysegul Dundar, Jun Gao, Andrew Tao, and Bryan Catanzaro. Progressive learning of 3d reconstruction network from 2d gan data. *IEEE Transactions on Pattern Analysis and Machine Intelligence*, 2023. 2
- [12] Jingwei Gao, Tianyang Shen, Zhen Wang, Weikai Chen, Kangxue Yin, Difan Li, Or Litany, Zan Gojcic, and Sanja Fidler. Get3d: A generative model of high quality 3d textured shapes learned from images. *arXiv preprint arXiv:2209.11163*, 2022. 2
- [13] J Hao, J Tang, J Zhang, et al. Portrait3d: 3d head generation from single in-the-wild portrait image. *arXiv preprint arXiv:2406.16710*, 2024. 2, 3, 4
- [14] Jianwen Jiang, Gaojie Lin, Zhengkun Rong, Chao Liang, Yongming Zhu, Jiaqi Yang, and Tianyun Zhong. Mobileportrait: Real-time one-shot neural head avatars on mobile devices. *arXiv preprint arXiv:2407.05712*, 2024. 1
- [15] Xuan Ju, Xian Liu, Xintao Wang, Yuxuan Bian, Ying Shan, and Qiang Xu. Brushnet: A plug-and-play image inpainting model with decomposed dual-branch diffusion. *arXiv preprint arXiv:2403.06976*, 2024. 5
- [16] Animesh Karnewar, Andrea Vedaldi, David Novotny, and Niloy J Mitra. Holodiffusion: Training a 3d diffusion model using 2d images. In *Proceedings of the IEEE/CVF Conference on Computer Vision and Pattern Recognition*, pages 18423–18433, 2023. 2
- [17] Tobias Kirschstein, Simon Giebenhain, and Matthias Nießner. Diffusionavatars: Deferred diffusion for high-fidelity 3d head avatars. In *Proceedings of the IEEE/CVF Conference on Computer Vision and Pattern Recognition*, 2024. 3
- [18] Xueting Li, Shalini De Mello, Sifei Liu, Koki Nagano, Umar Iqbal, and Jan Kautz. Generalizable one-shot 3d neural head avatar. *Advances in Neural Information Processing Systems*, 36, 2024. 1
- [19] Xiaoxiao Long, Yuan-Chen Guo, Cheng Lin, Yuan Liu, Zhiyang Dou, Lingjie Liu, Yuexin Ma, Song-Hai Zhang, Marc Habermann, Christian Theobalt, et al. Wonder3d: Single image to 3d using cross-domain diffusion. In *Proceedings of the IEEE/CVF Conference on Computer Vision and Pattern Recognition*, pages 9970–9980, 2024. 1, 7
- [20] Zhiyuan Ma, Xiangyu Zhu, Guo-Jun Qi, Zhen Lei, and Lei Zhang. Otavatar: One-shot talking face avatar with controllable tri-plane rendering. In *Proceedings of the IEEE/CVF Conference on Computer Vision and Pattern Recognition*, pages 16901–16910, 2023. 1
- [21] Ashkan Mirzaei, Tristan Aumentado-Armstrong, Marcus A Brubaker, Jonathan Kelly, Alex Levinshtein, Konstantinos G Derpanis, and Igor Gilitschenski. Reference-guided controllable inpainting of neural radiance fields. In *Proceedings of the IEEE/CVF International Conference on Computer Vision*, pages 17815–17825, 2023. 2
- [22] Ashkan Mirzaei, Tristan Aumentado-Armstrong, Konstantinos G Derpanis, Jonathan Kelly, Marcus A Brubaker, Igor Gilitschenski, and Alex Levinshtein. Spin-nerf: Multiview segmentation and perceptual inpainting with neural radiance fields. In *Proceedings of the IEEE/CVF Conference on Computer Vision and Pattern Recognition*, pages 20669–20679, 2023.
- [23] Ashkan Mirzaei, Riccardo De Lutio, Seung Wook Kim, David Acuna, Jonathan Kelly, Sanja Fidler, Igor Gilitschenski, and Zan Gojcic. Reffusion: Reference adapted diffusion models for 3d scene inpainting. *arXiv preprint arXiv:2404.10765*, 2024. 2

- [24] B. Poole, A. Jain, J.T. Barron, and B. Mildenhall. Dreamfusion: Text-to-3d using 2d diffusion. *arXiv preprint arXiv:2209.14988*, 2022. 1, 2
- [25] Ben Poole, Ajay Jain, Jonathan T Barron, and Ben Mildenhall. Dreamfusion: Text-to-3d using 2d diffusion. *arXiv preprint arXiv:2209.14988*, 2022. 2, 3
- [26] Guocheng Qian, Jinjie Mai, Abdullah Hamdi, Jian Ren, Aliaksandr Siarohin, Bing Li, Hsin-Ying Lee, Ivan Skokhodov, Peter Wonka, Sergey Tulyakov, et al. Magic123: One image to high-quality 3d object generation using both 2d and 3d diffusion priors. *arXiv preprint arXiv:2306.17843*, 2023. 1, 2
- [27] Pradyumna Reddy, Ismail Elezi, and Jiankang Deng. G3dr: Generative 3d reconstruction in imagenet. In *Proceedings of the IEEE/CVF Conference on Computer Vision and Pattern Recognition*, pages 9655–9665, 2024. 2
- [28] Ruizhi Shao, Youxin Pang, Zerong Zheng, Jingxiang Sun, and Yebin Liu. Human4dit: Free-view human video generation with 4d diffusion transformer. *arXiv preprint arXiv:2405.17405*, 2024. 2
- [29] Jingxiang Sun, Bo Zhang, Ruizhi Shao, Lizhen Wang, Wen Liu, Zhenda Xie, and Yebin Liu. Dreamcraft3d: Hierarchical 3d generation with bootstrapped diffusion prior. In *The Twelfth International Conference on Learning Representations*, 2024. 2, 7
- [30] J. Tang, T. Wang, B. Zhang, T. Zhang, R. Yi, L. Ma, and D. Chen. Make-it-3d: High-fidelity 3d creation from a single image with diffusion prior. *arXiv preprint arXiv:2303.14184*, 2023. 1, 2
- [31] J. Tang, Y. Zeng, K. Fan, X. Wang, B. Dai, K. Chen, and L. Ma. Make-it-vivid: Dressing your animatable biped cartoon characters from text. In *Proceedings of the IEEE/CVF Conference on Computer Vision and Pattern Recognition*, pages 6243–6253, 2024. 1, 2
- [32] Ayush Tewari, Tianwei Yin, George Cazenavette, Semon Rezhikov, Josh Tenenbaum, Frédo Durand, Bill Freeman, and Vincent Sitzmann. Diffusion with forward models: Solving stochastic inverse problems without direct supervision. *Advances in Neural Information Processing Systems*, 36: 12349–12362, 2023. 2
- [33] Dongqing Wang, Tong Zhang, Alaa Abboud, and Sabine Süsstrunk. Innerf360: Text-guided 3d-consistent object inpainting on 360-degree neural radiance fields. In *Proceedings of the IEEE/CVF Conference on Computer Vision and Pattern Recognition*, pages 12677–12686, 2024. 2
- [34] Ethan Weber, Aleksander Holynski, Varun Jampani, Saurabh Saxena, Noah Snavely, Abhishek Kar, and Angjoo Kanazawa. Nerfiller: Completing scenes via generative 3d inpainting. In *Proceedings of the IEEE/CVF Conference on Computer Vision and Pattern Recognition*, pages 20731–20741, 2024. 2
- [35] Yiqian Wu, Hao Xu, Xiangjun Tang, Hongbo Fu, and Xiaogang Jin. 3dportraitgan: Learning one-quarter headshot 3d gans from a single-view portrait dataset with diverse body poses. *arXiv preprint arXiv:2307.14770*, 2023. 1
- [36] Yiqian Wu et al. Portrait3d: Text-guided high-quality 3d portrait generation using pyramid representation and gans prior. *ACM Transactions on Graphics (TOG)*, 43(4):1–12, 2024. 1, 3, 7
- [37] Jing Xiang, Jian Yang, Yinda Deng, and Xin Tong. Gram-hd: 3d-consistent image generation at high resolution with generative radiance manifolds. *arXiv preprint arXiv:2206.07255*, 2022. 2
- [38] Jianfeng Xiang, Jiaolong Yang, Binbin Huang, and Xin Tong. 3d-aware image generation using 2d diffusion models. In *Proceedings of the IEEE/CVF International Conference on Computer Vision*, pages 2383–2393, 2023. 2
- [39] Sitao Xiang, Yuming Gu, Pengda Xiang, Mingming He, Koki Nagano, Haiwei Chen, and Hao Li. One-shot identity-preserving portrait reenactment. *arXiv preprint arXiv:2004.12452*, 2020. 1
- [40] Jiaxin Xie, Hao Ouyang, Jingtian Piao, Chenyang Lei, and Qifeng Chen. High-fidelity 3d gan inversion by pseudo-multi-view optimization. In *Proceedings of the IEEE/CVF Conference on Computer Vision and Pattern Recognition*, pages 321–331, 2023. 2
- [41] Shaoan Xie, Zhifei Zhang, Zhe Lin, Tobias Hinz, and Kun Zhang. Smartbrush: Text and shape guided object inpainting with diffusion model. In *Proceedings of the IEEE/CVF Conference on Computer Vision and Pattern Recognition*, pages 22428–22437, 2023. 1
- [42] You Xie, Hongyi Xu, Guoxian Song, Chao Wang, Yichun Shi, and Linjie Luo. X-portrait: Expressive portrait animation with hierarchical motion attention. In *ACM SIGGRAPH 2024 Conference Papers*, pages 1–11, 2024. 2
- [43] Zhangyang Xiong, Di Kang, Derong Jin, Weikai Chen, Linchao Bao, Shuguang Cui, and Xiaoguang Han. Get3dhuman: Lifting stylegan-human into a 3d generative model using pixel-aligned reconstruction priors. In *Proceedings of the IEEE/CVF International Conference on Computer Vision*, pages 9287–9297, 2023. 2
- [44] Shiyuan Yang, Xiaodong Chen, and Jing Liao. Uni-paint: A unified framework for multimodal image inpainting with pretrained diffusion model. In *Proceedings of the 31st ACM International Conference on Multimedia*, pages 3190–3199, 2023. 1
- [45] Zhenhui Ye, Tianyun Zhong, Yi Ren, Jiaqi Yang, Weichuang Li, Jiawei Huang, Ziyue Jiang, Jinzheng He, Rongjie Huang, Jinglin Liu, et al. Real3d-portrait: One-shot realistic 3d talking portrait synthesis. *arXiv preprint arXiv:2401.08503*, 2024. 1
- [46] Taoran Yi, Jiemin Fang, Junjie Wang, Guanjun Wu, Lingxi Xie, Xiaopeng Zhang, Wenyu Liu, Qi Tian, and Xinggang Wang. Gaussiandreamer: Fast generation from text to 3d gaussians by bridging 2d and 3d diffusion models. In *Proceedings of the IEEE/CVF Conference on Computer Vision and Pattern Recognition*, pages 6796–6807, 2024. 1, 2
- [47] Feng Yin, Yifan Zhang, Xiaoming Wang, Ting Wang, Xiaoyu Li, Yifan Gong, Yuchen Fan, Xiaodong Cun, Ying Shan, and Cengiz Oztireli. 3d gan inversion with facial symmetry prior. In *Proceedings of the IEEE/CVF Conference on Computer Vision and Pattern Recognition*, pages 342–351, 2023. 1, 3
- [48] Fei Yin, Yong Zhang, Xuan Wang, Tengfei Wang, Xiaoyu Li, Yuan Gong, Yanbo Fan, Xiaodong Cun, Ying Shan, Cengiz

- Oztireli, et al. 3d gan inversion with facial symmetry prior. In *Proceedings of the IEEE/CVF Conference on Computer Vision and Pattern Recognition*, pages 342–351, 2023. [2](#)
- [49] Xianfang Zeng, Xin Chen, Zhongqi Qi, Wen Liu, Zibo Zhao, Zhibin Wang, Bin Fu, Yong Liu, and Gang Yu. Paint3d: Paint anything 3d with lighting-less texture diffusion models. In *Proceedings of the IEEE/CVF Conference on Computer Vision and Pattern Recognition*, pages 4252–4262, 2024. [2](#)
- [50] Bowen Zhang, Yiji Cheng, Chunyu Wang, Ting Zhang, Jiaolong Yang, Yansong Tang, Feng Zhao, Dong Chen, and Baining Guo. Rodinhd: High-fidelity 3d avatar generation with diffusion models. *arXiv preprint arXiv:2407.06938*, 2024. [2](#)